An organosilicon-loaded plastic scintillator synthesized for neutron/gamma discrimination

Authors: Liu, Mr. Weirong, Shi, Dr. Pengcheng, Dr. Yingdu Liu, Zhu, Miss Zhiyun, Zhang, Miss Siyu, Bao, Dr. Jie, Dr. Xiaoping Ouyang, Liu, Dr. Yingdu

Date: 2025-06-04T16:13:18+00:00

Abstract

In this work, we report a scintillator used for neutron/gamma discrimination, which consists of a polyvinyltoluene matrix loaded with monomers of dimethoxydiphenylsilane (DDS), and fluor dyes, namely 2,5-diphenyloxazole and 7-diethylamino-4-methylcoumarin as the primary fluorophore and wavelength-shifting, respectively. The DDS is an organosilicon compound containing double benzene rings that facilitates fluorescence emission and radiation resistance. Several measurements were performed to explore the scintillators optical and detection properties, including ^{238}Pu-Be neutron radiation and relative light yield conducted by 137Cs gamma-ray source. It is found that the synthesized plastic scintillators are capable of excellently discriminating between neutron and gamma-rays. They exhibit a light output that are comparable to the commercial scintillator (EJ-200). The scintillators are low-cost productive, highly transparent, and somewhat soft but hard enough for post-production processing (machine cutting and polishing). This design may contribute a new strategy for highly efficient neutron/gamma discrimination organic scintillators.

Full Text

Preamble

An organosilicon-loaded plastic scintillator synthesized for neutron/gamma discrimination

Weirong Liu[1], Pengcheng Shi[2], Yingdu Liu[1],†, Zhiyun Zhu[1], Siyu Zhang[1], and Jie Bao[3],‡

[1]School of Materials Science and Engineering, Xiangtan University, Xiangtan 411105, People's Republic of China

[2]Xi'an Institute of Optics and Precision Mechanics of CAS, Xi'an 710119, People's Republic of China
[3]Nuclear Data Key Laboratory, China Institute of Atomic Energy, Beijing 102413, People's Republic of China

In this work, we report a novel scintillator for neutron/gamma discrimination comprising a polyvinyltoluene matrix loaded with dimethoxydiphenylsilane (DDS) monomers and fluor dyes—2,5-diphenyloxazole (PPO) as the primary fluorophore and 7-diethylamino-4-methylcoumarin (MDAC) as the wavelength shifter. DDS is an organosilicon compound containing dual benzene rings that enhances fluorescence emission and radiation resistance. We conducted comprehensive measurements to characterize the scintillators' optical and detection properties, including tests with a ^{238}Pu-Be neutron source and relative light yield measurements using a ^{137}Cs gamma-ray source. The synthesized plastic scintillators demonstrate excellent neutron/gamma discrimination capability with light output comparable to commercial EJ-200 scintillators. These scintillators offer low-cost production, high optical transparency, and optimal mechanical properties—sufficiently soft for elasticity yet hard enough for post-production machining and polishing. This design presents a promising new strategy for developing highly efficient neutron/gamma discrimination organic scintillators.

Keywords: Neutron detection, Plastic scintillation, Pulse shape discrimination, Polymethyl-methacrylate, Polystyrene

Introduction

Organic scintillator-based neutron detection has served as an effective tool in nuclear and particle physics experiments for decades, particularly in high-radiation environments [1–3]. However, neutron measurements are invariably accompanied by gamma rays generated through neutron activation of surrounding materials. Consequently, the ability to distinguish between neutrons and gamma rays—known as pulse shape discrimination (PSD) [4,5]—is essential for reliable neutron spectroscopy using organic scintillators, especially when detecting high-energy neutrons in gamma-ray backgrounds [6]. For many years, neutron detection has predominantly relied on ^{3}He proportional counters due to their excellent gamma rejection and high detection efficiency for thermal neutrons [7–9]. However, the extremely high cost of ^{3}He has limited its widespread deployment and stimulated intensive research into alternative, more economical materials. Among PSD-capable organic scintillators, plastic scintillators have recently emerged as promising candidates for large-scale scientific infrastructure, border security systems, and reactor monitoring applications [10]. Unlike single crystals, which are constrained by high manufacturing costs, or liquid scintillators, which suffer from toxicity, flammability, and handling challenges for large-area detectors, plastic scintillators offer distinct advantages including low production cost, inherent safety, ease of fabrication, and the ability to be manufactured in customizable geometries [11,12].

The most widely used plastic scintillators are ternary systems composed of polystyrene (PS) or polyvinyltoluene (PVT) matrices doped with primary fluorophores and secondary wavelength shifters [13–15]. These aromatic hydrocarbon polymers contain benzene rings bonded to methyl (CH_3–) and vinyl (CH_2=CH–) groups. When irradiated by high-energy particles, molecular chains in such polymers undergo damage through scission and cross-linking [1], altering their chemical structure and generating free radicals that form color centers [16,17]. These radiation-induced transformations correlate with bond dissociation energies in the polymer backbone: 3.59 eV for C–C bonds, 3.71 eV for C–O bonds, and 4.61 eV for Si–O bonds [17]. Polysiloxane, also known as organosilicon base with a backbone of alternating Si–O–Si bonds and organic substituents, exhibits high bond energy and excellent radiation resistance. Studies demonstrate that polysiloxane-based scintillators show no color yellowing at radiation doses of 100 kGy [18]. These scintillators are capable of discriminating neutrons in the presence of gamma-ray background using time-of-flight (TOF) method [19] or PSD technique [20]. However, they are soft due to the elastic nature. Although cross-linking strategies can improve fluorescence scintillation [21], they exhibit inherently inferior PSD performance compared to conventional PS/PVT-based systems.

In this work, we have developed a novel PSD organic scintillator that combines the advantages of both pure PVT and polysiloxane matrices through copolymerization of DDS monomers with PVT resins, doping with PPO and MDAC as the primary fluorophore and wavelength-shifting component, respectively. Through low-density self-polymerization, the DDS monomers form linear polysiloxane segments that interpenetrate the PVT cross-linked network, resulting in bulk scintillators with some elasticity while retaining adequate rigidity for mechanical machining. The synthesized scintillators are highly transparent, cost-effective, and outstanding in PSD performance. Such advantages make this scintillator a promising candidate for large-scale radiation detection applications.

II. Samples Fabrication and Characterization

Vinyltoluene monomers (C_9H_{10}, >98%, m- and p-mixture, containing stabilizer TBC) were purchased from TCI Chemicals (Shanghai) Industrial Development Co., Ltd. DDS, MDAC, and the initiator 2,2'-Azobis(2-methylpropionitrile) (AIBN, >98%) were obtained from Shanghai Macklin Biochemical Co., Ltd. PPO was purchased from Shanghai YuanYe Biotechnology Co., Ltd., and divinylbenzene (DVB, containing stabilizer) was obtained from Meryer (Shanghai) Chemical Technology Co., Ltd.

The synthesis procedure for the scintillator samples is similar to that described in our previous work [13]. Prior to sample preparation, the vinyltoluene monomers and divinylbenzene were passed through an aluminum oxide column to remove stabilizers, then mixed and stirred at room temperature for three minutes. The mixture was sonicated until a homogeneous and clear solution was obtained. Subsequently, fluorophores (30 wt% PPO, 0.2 wt% MDAC,

where “wt%” denotes weight percent), radical polymerization initiator (0.05 wt% AIBN), and cross-linking agent (2 wt% DVB) were added to the mixture, stirred for an additional 2–5 minutes, and transferred to flat-bottom glass vials for ultrasonication until the dopants were completely dissolved. The mixed solution was poured into glass vials and treated repeatedly at least three times by a process of fast freezing with liquid nitrogen, vacuum degassing (3–5 min), and thawing at room temperature to completely remove dissolved oxygen. The vials were sealed in an oxygen-free atmosphere and heated in a thermostat to promote radical thermal polymerization.

To prevent explosive polymerization, the thermostat temperature was maintained at 50.0 °C for two days, then slowly increased from 80.0 °C to 110.0 °C at a rate of 3 °C/h and held for 24 h. To prevent crack and bubble formation during annealing, the polymers were slowly cooled to room temperature at 3 °C/h, then placed in a constant temperature environment at 50.0–60.0 °C for internal stress release. Plastic scintillators with varying DDS content (RK1–RK5 corresponding to 20, 25, 30, 35, and 40 wt% DDS, respectively) were obtained from the thermostat by carefully breaking the vials after cooling to room temperature. The resulting samples measured approximately 20.0 mm in diameter and 10.0 mm in thickness.

The scintillators were cut and polished to match the dimensions of control samples (EJ-200, EJ-276). Thickness differences between samples were measured to be no more than 100 μm using a Mitutoyo micrometer (Mitutoyo Corp.). Shore hardness was evaluated using a portable digital durometer (Shore A hardness meter, Taizhou AI Measurement Instrument Co., Ltd.), with five equidistant points measured on a flat side of each sample and averaged to obtain the hardness value. Elastic recovery testing and excitation-emission spectra were performed using a metallographic microscope (BX53M, Olympus Corp.) and an FLS1000 fluorescence spectrometer (Edinburgh Instruments), respectively. Ultraviolet-visible transmission spectra were recorded using a UV-Vis spectrophotometer (PerkinElmer Lambda 750) over an emission wavelength range of 250–800 nm. Thermal decomposition behavior was studied from 30 °C to 800 °C using a thermogravimetric analyzer (STA 449 F3 Jupiter, Netzsch GmbH, Germany), and Fourier-transform infrared spectra (FTIR) were obtained using a Fourier transform infrared spectrometer (Nicolet 6700, Thermo Fisher Scientific, USA) to analyze structure and functional groups.

The scintillators were irradiated with a 20 Ci ^{238}Pu-Be neutron source installed at the University of South China to study their PSD performance using an 8-channel 14-bit 500 MS/s flash ADC waveform digitizer (CAEN DT5730). All samples were wrapped in three layers of polytetrafluoroethylene (PTFE) tape on every surface except the one coupled to a photomultiplier tube (PMT, Hamamatsu H1949-51) with optical dimethyl silicone (Dow Corning, PMX-200). Signals collected from the PMT anode were converted to digital waveforms and analyzed by CAEN DPP-PSD firmware, which combines digital QDC (charge integration) and discriminator functions for particle identification. A ^{60}Co source

(1.17 MeV, 1.33 MeV) in tandem with ^{137}Cs (662 keV) was used for electron equivalent energy calibration by Gaussian fitting to the Compton edge position of each source. Light output (LO) was determined using the maximum position of the Compton edge in the ^{137}Cs pulse height spectra and compared with commercially available three-year-stored EJ-200 to obtain relative LO. To explore sample stability in terms of relative LO and PSD performance, measurements were carried out three times at 2 days, 96 days, and 172 days after preparation. Conditions including digitizer settings, PMT operation at –1600 V by high voltage power supply (ISEG Cor.), 10 cm distance from neutron source to samples, and lead brick shielding were kept constant to ensure consistency between measurements.

III. Results and Discussion

A. Physical Properties

DDS is a cost-effective organosilicon compound with dual benzene rings that efficiently dissolves organic dyes. Organosilicon compounds have demonstrated superior radiation resistance compared to conventional PVT- or PS-based scintillators [1,22–25]. Therefore, we expect PVT-DDS based PSD organic scintillators to exhibit enhanced radiation stability relative to pure PVT-based scintillators. The aromatic matrices (PVT and DDS) exhibit specific optical properties: they emit fluorescence primarily in the ultraviolet region (250–380 nm) [26], with absorption spectra showing noticeable absorption starting around 380 nm and increasing sharply below 350 nm [12]. Specifically, PVT exhibits excitation and emission peaks at 266 nm and 310 nm, respectively, while DDS shows corresponding peaks at 302 nm and 353 nm (Fig. S1, Supplementary Materials). To minimize self-absorption by the matrix, primary fluorophore PPO is added to absorb photons from matrix emission and emit photons with a peak at 393 nm. To maintain scintillation in the blue-green region of the optical spectrum that matches PMT sensitivity, wavelength-shifter MDAC is chosen to shift emission to 410–500 nm. As the primary fluorophore, PPO has high solubility in aromatic solvents, while MDAC, a secondary dye with high light output, is routinely used in plastic preparation. This PPO-MDAC dye pair likely contributes to excellent PSD capability in PVT-DDS based scintillators from the perspective of fundamental energy transfer principles [27].

With 20–40 wt% DDS, the synthesized scintillators are colorless and optically transparent without yellowing or surface dye precipitation visible to the naked eye even six months after preparation (Fig. 1

(a)). However, when DDS content exceeds 40 wt%, microcracks, cracking, and color yellowing are observed (Fig. 1(b)-Top). In contrast to pure PVT-based samples (0 wt% DDS), scintillators containing 10–30 wt% DDS and 50 wt% PPO remain optically transparent after 15 days of storage (Fig. 1(b)-Bottom), revealing significantly improved fluorophore dissolution stability afforded by DDS monomers. This improvement may be understood through molecular iso-

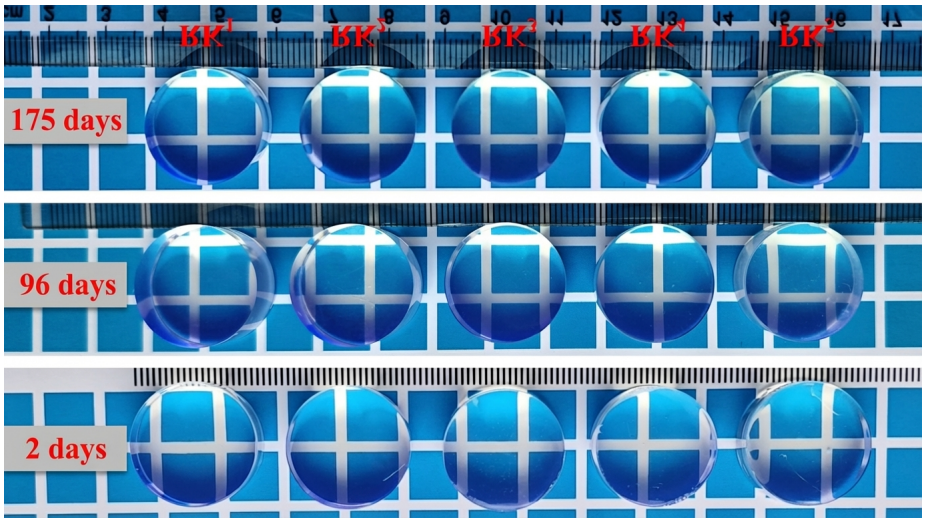

Figure 1: Figure 1

lation within network subdomains constructed by functional monomers, where spatial separation of fluorophores minimizes intermolecular interactions. Combined with our previous research [21], we conclude that small amounts of functional monomers loaded into the host scintillator matrix and participating in cross-linked network formation consistently improve dye dispersion and prevent aggregation.

The mechanical hardness of scintillators RK1–RK5 was measured as $45.5\$\pm0.8HD, 41.4\pm0.5HD, 39.7\pm0.3HD, 39.3\pm0.9HD, and37.2\pm\$0.5$ HD, respectively, showing a general decrease with increasing DDS content. As shown in Fig. 2

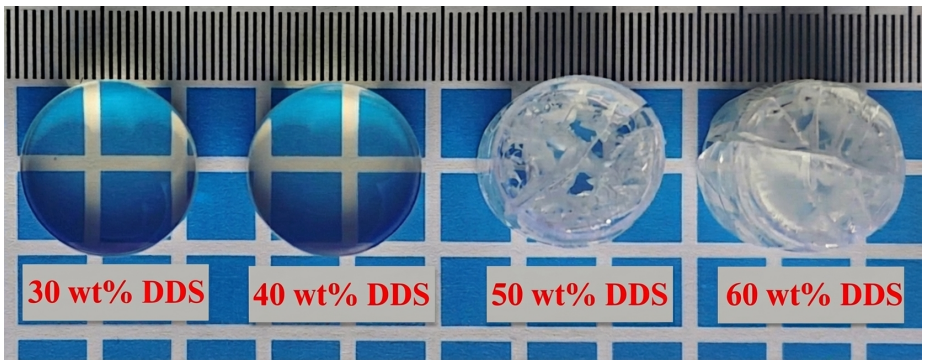

Figure 2: Figure 2

, the 30 wt% DDS composite exhibited no significant spectral alterations in

FTIR spectra compared to the pure PVT matrix (0 wt% DDS), except for a distinct absorption band at 1065.59 cm^{-1} corresponding to Si–O–Si vibration. The absence of new characteristic peaks or peak shifts suggests that DDS incorporation does not chemically modify the polymer chain structure but rather establishes a physically compatible blended system.

We speculate that during thermal polymerization, low-molecular-weight siloxane chains derived from DDS monomers were incorporated into the PVT-based cross-linked network. This structural integration, combined with the inherent elasticity of DDS siloxane components, likely contributes to reduced mechanical hardness. Such reduction is not necessarily detrimental from the perspective of elastic recovery properties. To confirm this, a blunt needle with 0.79 mm diameter was used to press the scintillator sample (30 wt% DDS) for one minute. The time evolution of surface morphology for sample RK3 is shown in Fig. 3[FIGURE:3] and Fig. S2 (Supplementary Materials). The initial indentation exhibited cylindrical geometry with 1.5 mm depth. Remarkably, within 30 seconds post-compression, the indentation underwent near-complete recovery to a planar surface. After 60 seconds, minimal residual deformation or surface extrusion traces were observed, confirming that DDS introduction imparts elastic recovery properties to the scintillator. This phenomenon may be attributed to high mobility of siloxane main chains facilitated by exceptionally low energy barriers for Si–O–Si bond bending and torsional motions [28].

Thermal stability was assessed via thermogravimetric analysis (TGA) under protective nitrogen atmosphere, with temperature increased at 10 °C/min from 30 °C to 800 °C. Results are shown in Fig. 4[FIGURE:4]. No mass loss occurred below 120 °C. The synthesized scintillators exhibited similar thermogravimetric profiles during the first degradation stage (120–260 °C), where samples underwent inter- or intrachain reactions generating low-molecular-weight products including volatile compounds, linear oligomers, and fluorophores (PPO, MDAC). Compared to the 0 wt% DDS scintillator (decomposition temperature 160 °C), DDS-containing scintillators began decomposing at lower temperatures, perhaps due to phase-separated domains created between DDS and PVT constituents. Above 210 °C, thermal degradation rate showed slight dependence on DDS content in a complex manner requiring future investigation. In the second stage (260–380 °C), DDS-containing samples exhibited faster weight loss than pure PVT-based scintillators, indicating reduced thermal stability of DDS short-chain structures. During the third stage (380–800 °C), degradation continued with 2–5% solid residue consisting primarily of SiOC carbonaceous substance from mineralization [29].

B. Optical Performance

The synthesized scintillators utilize PVT and DDS as matrices. Critically, the emission spectra of both PVT and DDS matrices overlap significantly with the absorption spectrum of fluorophore PPO, enabling efficient Förster resonance energy transfer (FRET) from matrices to PPO. To simultaneously excite

both matrices, a 270 nm UV source was selected. This wavelength lies well below the 310–330 nm absorption peaks of both PPO and MDAC fluorophores, thereby minimizing direct fluorophore excitation and allowing specific investigation of resonance energy transfer from excited matrices. Figure 5(a)[FIGURE:5] presents the excitation-emission matrix of RK3 scintillator (30 wt% DDS). Under 270 nm excitation, its emission spectrum (scanned from 400–600 nm) shows a distinct 434 nm peak. The excitation spectrum over 250–400 nm was monitored at 434 nm wavelength. The prominent emission peak at 434 nm signifies characteristic fluorescence of MDAC dye, and its presence under 270 nm excitation provides strong evidence for efficient energy transfer from excited matrices to MDAC dye.

Photoluminescence (PL) spectra excited at 270 nm are shown in Fig. 5FIGURE:5 and Fig. S3 (Supplementary Materials). Increasing DDS content promotes π–π stacking of benzene moieties, enhancing exciplex formation and resulting in broadened emission peaks with 10–30 nm red shifts. PL intensity initially rises with DDS concentration but declines above 30 wt% DDS. At high concentrations, fluorescence emission is likely dominated by aggregation-caused quenching (ACQ), where dense π–π stacking creates compact molecular proximity. This facilitates electron energy level rearrangement in the matrix, primarily through splitting of ground-state and first excited-state levels. Consequently, concentration-dependent PL intensity correlates with scintillator optical transparency, as both phenomena originate from photon loss mechanisms in aggregated systems.

Optical transparency of the scintillators is very high (Fig. 5(c)[FIGURE:5]). All samples exhibit transmittance between 70% and 87%, comparable to commercial scintillator EJ-276 (Fig. S4, Supplementary Materials). Within the visible spectrum, transmittance initially increases with DDS content up to 30 wt%. However, further DDS increases lead to decreased transmittance. This non-monotonic behavior is attributed to two factors: self-absorption within the matrix material and dye molecule aggregation at higher DDS concentrations. Below 30 wt% DDS, monomers were sparsely dispersed; most did not participate in thermal polymerization and acted as photon scattering centers, reducing transparency. As DDS approaches 30 wt%, dispersed monomers polymerized into linear-chain segments, enhancing transparency. However, above 30 wt% DDS, high benzene ring density promoted strong π–π stacking interactions that induced fluorophore aggregation [30]. At these concentrations, numerous low-molecular-weight DDS chains embedded within the cross-linked PVT network created phase-separated domains with mismatched plastic deformation behaviors. This structural incompatibility generated interfacial shear stresses and microcracks at phase boundaries (Fig. 1(b)-Top), causing observed transparency reduction.

C. PSD and Relative Light Output

We studied PSD performance of the synthesized scintillators using a ^{238}Pu-Be source. The PSD method identifies particles based on different proportions of prompt and delayed components in scintillation pulses. When energetic particles pass through a scintillator, π electrons of scintillator molecules are ionized and recombine to produce both singlet and triplet excited states, which then promptly de-excite to the lowest singlet (S_1) and triplet (T_1) states [31]. Transition from S_1 to ground state (S_0) with fluorescence emission on a timescale of 10^{-9}–10^{-8} s produces the prompt component. Direct transition from T_1 to S_0 is spin-forbidden; instead, a bimolecular triplet–triplet annihilation process ($T_1 + T_1 \rightarrow S_1 + S_0$), known as TTA, occurs kinematically with subsequent S_1 de-excitation ($S_1 \rightarrow S_0 + h$) over a longer timescale (10^{-4} s), producing the delayed component. T_1 state density depends on the ionizing power of incident particles. For a given incident energy, heavy charged particles produce more T_1 states per unit path length than light particles, resulting in a more pronounced slow scintillation component. This difference in integrated charge ratio between prompt and delayed components forms the basis of PSD.

We evaluated PSD capability using the charge integration method [32]. For each digital waveform, integrations over a short-time gate (Q_{short}, fast component) and long-time gate (Q_{total}) yield the PSD parameter:

$$P_{SD} = 1 - \frac{Q_{short}}{Q_{total}}$$

where Q_{short} is the charge integral from waveform start to prompt peak, and Q_{total} represents the full-waveform integral. Two-dimensional plots of P_{SD} versus Q_{total} are shown in Fig. 6[FIGURE:6] and Fig. S5 (Supplementary Materials) for prepared scintillators (RK1–RK5 and 0 wt% DDS sample) two days after synthesis, alongside EJ-276. Excellent separation between neutron and gamma-ray signals is observed. The locus with higher P_{SD} values corresponds to neutrons, while lower P_{SD} values correspond to gamma rays. Notably, neutron and gamma bands exhibit distinct curvature, potentially arising from PMT non-linearity under high-voltage operation (Fig. S6, Supplementary Materials) [33,34]. The capability to separate neutrons from gamma rays is quantified by the figure of merit (FOM), defined as FOM = S/(σ_γ + σn), *where S represents separation between gamma and neutron distribution peaks, and* $\sigma\gamma$ (σn) *denotes full width at half-maximum (FWHM) of gamma (neutron) peaks in one-dimensional P*{SD} distribution. These parameters are obtained through Gaussian fitting. Consequently, PSD FOM depends on two factors: neutron/gamma peak separation (S) and their respective widths. Increasing light output reduces FWHM of both distributions, thereby enhancing PSD FOM [27].

To quantitatively assess PSD capability dependence on DDS concentration, we extracted P_{SD} values within Q_{total} range of 0.2–1.2 MeVee (MeV elec-

tron equivalent energy) from 2D distributions. Figure 7(a)[FIGURE:7] plots calculated FOM values against DDS concentration, while Fig. 7(b) shows FOM values calculated within each Q_{total} bin (in MeVee) up to 1.2 MeVee for prepared scintillators (black dots). As clearly demonstrated in Fig. 7(b), each scintillator achieves superior neutron/gamma separation with FOM of 1.27 at Q_{total} values down to 0.15 MeVee. This value of 1.27 is generally recognized as the FOM threshold for efficient pulse shape discrimination [11].

We studied light output of prepared scintillators using a ^{137}Cs source by comparing Compton edge positions in their pulse height spectra with those of EJ-200 standard (Fig. S7, Supplementary Materials). As shown in Fig. 7(c)[FIGURE:7], light output relative to EJ-200 exhibits an overall decreasing trend within calculated uncertainties as DDS monomer concentration increases. Conversely, neutron/gamma PSD capability, quantified by FOM, shows slight concentration-dependent enhancement before reaching a plateau (Fig. 7(a)[FIGURE:7]). This apparent inverse correlation between PSD performance and light output likely arises from formation of a more efficient triplet (T_1) state energy transfer network. This network emerges from gradual substitution of PVT with DDS, increasing benzene ring density required for triplet energy migration. Furthermore, enhanced fluorophore dissolution facilitated by DDS incorporation likely affects local T_1 excitation density and efficiency of the TTA process governing neutron/gamma separation parameter S.

Long-term stability was evaluated through repeat measurements at 96 and 172 days after synthesis (Fig. 7(a)[FIGURE:7] and (c)[FIGURE:7]). After approximately six months of aging, synthesized scintillators exhibited 9–16% reductions in FOM and 27–41% reductions in light output relative to initial values. This degradation highlights a significant challenge. While DDS incorporation offers potential advantages in radiation resistance and PSD performance, observed aging effects—likely stemming from fluorophore aggregation, potential matrix instability at higher DDS loadings (as suggested by Fig. 1(b)

), or chemical degradation pathways—currently limit practical long-term utility of these materials. Addressing this stability issue, potentially through optimized fluorophore selection, stabilization additives, or refined matrix composition, is crucial for realizing the promising PSD performance of PVT-DDS based scintillators in demanding applications.

IV. Summary

Organic scintillators based on PS and PVT are widely used in many fields, from nuclear physics experiments to safeguard equipment. However, these materials suffer from poor radiation resistance. Breaking of C–C and C–H bonds generates free radicals and hydrogen release from the polymer, causing color yellowing and reductions in light yield and transparency. One approach to circumvent this problem is to replace or partially replace these materials with polysiloxane polymers having higher radiation hardness.

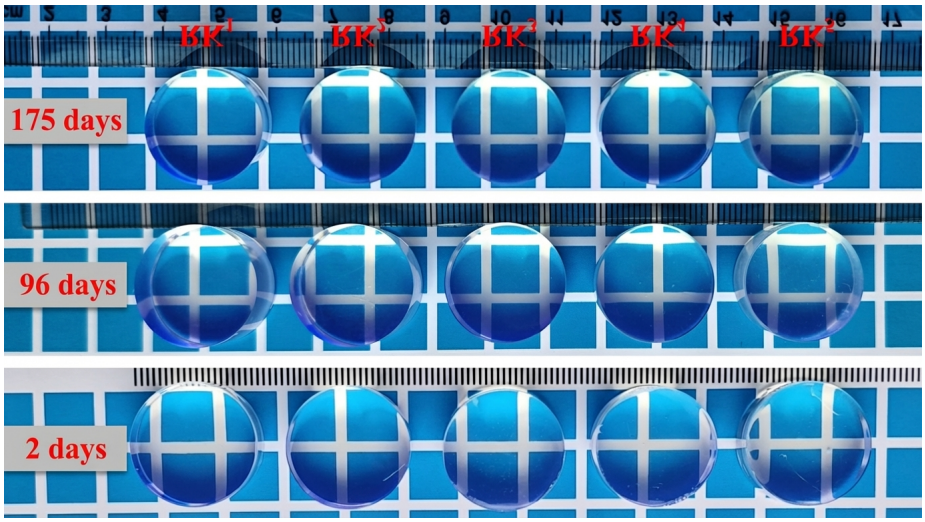

Figure 3: Figure 1

In this work, we successfully developed a novel elastic scintillator by incorporating 20–40 wt% siloxane compound DDS into the PVT matrix for neutron/gamma discrimination. The obtained organosilicon-loaded plastic scintillators comprise a mixture of PVT and siloxane-based matrix (DDS). They are transparent, mechanically hard enough for machining and polishing, and allow excellent discrimination of neutrons from background gamma rays. Performance characterization shows that DDS addition imparts elasticity and improves dye molecule solubility by preventing aggregation. While DDS-PVT based scintillators exhibit excellent PSD performance, they also show decreased light yield (86–98% relative to EJ-200) with increasing DDS concentration (RK1–RK5), implying that radioluminescence in such scintillators is less favorable than in PVT-based scintillators. Measurements at different times after preparation indicate that stability in terms of PSD and light output still requires improvement. Our future work will focus on investigating cross-linked networks in scintillators synthesized through copolymerization and homopolymerization, aiming to understand singlet and triplet exciton migration required for efficient PSD capability in organosilicon-loaded scintillators. Nevertheless, this newly designed organosilicon-loaded plastic scintillator is promising for fabrication of next-generation neutron detectors used under high-dose irradiation.

Acknowledgments

All authors contributed to this article. The design and preparation of scintillators were performed by Weirong Liu, Yingdu Liu, and Jie Bao. Experimental measurements were conducted by Weirong Liu, Zhiyun Zhu, and Siyu Zhang. Data analysis was completed by Weirong Liu and Pengcheng Shi. Weirong Liu

and Pengcheng Shi wrote the first draft, and all authors commented on previous versions. All authors have read and approved the final manuscript.

References

[1] Yu.N. Kharzheev, Radiation hardness of organic based detectors and scintillation optical fibers. *Phys. Part. Nucl.* **50**(1), 42–76 (2019). doi:10.1134/S1063779619010027

[2] K. Li, J.R. Zhou, X.-D. Wang et al., Study of a nTHGEM-based thermal neutron detector. *Chin. Phys. C* **40**, 076002 (2016). doi:10.1088/1674-1137/40/7/076002

[3] D. Zhao, X.W. Liang, P.K. Cai et al., Design and performance evaluation of a large field-of-view dual-particle time-encoded imager based on a depth-of-interaction detector. *Nucl. Sci. Tech.* **35**, 67 (2024). doi:10.1007/s41365-024-01416-2

[4] J.Q. Faisan, J. Lou, Z. Li et al., A pulse shape discrimination study of CsI(Tl) crystal with ^{6}He beam. *Nucl. Sci. Tech.* **21**(1), 35–38 (2010). doi:10.13538/j.1001-8042/nst.21.35-38

[5] S.X. Liu, W. Zhang, Z.H. Zhang, Performance of real-time neutron/gamma discrimination methods. *Nucl. Sci. Tech.* **34**(1), 8 (2023). doi:10.1007/s41365-022-01160-5

[6] Y.Q. Zhang, L.Q. Hu, G.Q. Zhong et al., Development of a high-speed digital pulse signal acquisition and processing system based on MTCA for liquid scintillator neutron detector on EAST. *Nucl. Sci. Tech.* **34**, 150 (2023). doi:10.1007/s41365-024-01416-2

[7] R.C. Runkle, A. Bernstein, P.E. Vanier, Securing special nuclear material: Recent advances in neutron detection and their role in nonproliferation. *J. Appl. Phys.* **108**(11), 111101 (2010). doi:10.1063/1.3503495

[8] R.T. Kouzes, A.T. Lintereur, E.R. Siciliano, Progress in alternative neutron detection to address the helium-3 shortage. *Nucl. Instrum. Meth. Phys. Res. A* **784**, 172–175 (2015). doi:10.1016/j.nima.2014.10.046

[9] S. Li, X. Ai, Z. Yu et al., Assessment of tritium monitoring for radiation environment around typical nuclear power plants in China. *J. Rad. Nucl. Chem.* **332**(7), 2581–2588 (2023). doi:10.1007/s10967-023-08939-9

[10] H. Nakano, T. Katabuchi, G. Rovira et al., Development of a neutron beam monitor with a thin plastic scintillator for nuclear data measurement using spallation neutron source. *J. Nucl. Sci. Tech.* **59**(12), 1499–1506 (2022). doi:10.1080/00223131.2022.2067598

[11] N. Zaitseva, B.L. Rupert, I. Pawełczak et al., Plastic scintillators with efficient neutron/gamma pulse shape discrimination. *Nucl. Instrum. Meth. Phys. Res. A* **668**, 88–93 (2012). doi:10.1016/j.nima.2011.11.071

[12] N.P. Zaitseva, A.M. Glenn, A.N. Mabe et al., Recent developments in plastic scintillators with pulse shape discrimination. *Nucl. Instrum. Meth. Phys. Res. A* **889**, 97–104 (2018). doi:10.1016/j.nima.2018.01.093

[13] Y.Y. Liang, Y.D. Liu, P.S. Wang et al., Optical transmittance and pulse shape discrimination of polystyrene/poly(methyl methacrylate)-based plastic scintillators. *Nucl. Sci. Tech.* **36**, 9 (2025). doi:10.1007/s41365-024-01577-0

[14] F. Bisaro, A. Inial, J. Gatignol et al., Plastic scintillators with 1-phenyl-3-(mesityl)-2-pyrazoline as unique fluorophore for efficient neutron/gamma pulse shape discrimination. *Nucl. Instrum. Meth. Phys. Res. A* **1030**, 166469 (2022). doi:10.1016/j.nima.2022.166469

[15] G.H.V. Bertrand, M. Hamel, S. Normand et al., Pulse shape discrimination between (fast or thermal) neutrons and gamma rays with plastic scintillators: The art of discrimination. *Nucl. Instrum. Meth. Phys. Res. A* **776**, 114–128 (2015). doi:10.1016/j.nima.2014.12.024

[16] Y. Zhang, R. Fan, Y. Yu et al., Radiation hardness study of BC408 plastic scintillator under 80 MeV proton beam irradiations. *Nucl. Instrum. Meth. Phys. Res. B* **548**, 165247 (2024). doi:10.1016/j.nimb.2024.165247

[17] A. Quaranta, S.M. Carturan, T. Marchi et al., Optical and scintillation properties of polydimethyl-diphenylsiloxane based organic scintillators. *IEEE Trans. Nucl. Sci.* **57**(2), 891–900 (2010). doi:10.1109/TNS.2010.2042817

[18] P. Zhmurin, Radiation-hard plastic scintillator with increased mechanical strength. *Funct. Mater.* **22**, 280–285 (2015). doi:10.15407/fm22.02.280

[19] S. Carturan, A. Quaranta, T. Marchi et al., Novel polysiloxane-based scintillators for neutron detection. *Radia. Protec. Dos.* **143**(2-4), 471–476 (2011). doi:10.1093/rpd/ncq403

[20] T. Marchi, F. Pino, C.L. Fontana et al., Optical properties and pulse shape discrimination in siloxane-based scintillation detectors. *Sci. Rep.* **9**(1), 9154 (2019). doi:10.1038/s41598-019-45630-8

[21] F. Chen, J. Li, L. Liu et al., Influence of a cross-linker agent on mechanical and other properties of polysiloxane based scintillators. *Nucl. Instrum. Meth. Phys. Res. A* **1067**, 169668 (2024). doi:10.1016/j.nima.2024.169668

[22] M. Bowen, S. Majewski, D. Pettey et al., A new radiation-hard plastic scintillator. *IEEE Trans. Nucl. Sci.* **36**(1-2), 562 (1989). doi:10.1016/0168-9002(89)90657-8

[23] V.M. Feygelman, J.K. Walker, J.P. Harmon, Polysiloxane-based scintillators: 1,1,4,4-tetraphenylbutadiene. *Nucl. Instrum. Meth. Phys. Res. A* **295**(1-2), 94–98 (1990). doi:10.1016/0168-9002(90)90426-7

[24] V.M. Feygelman, J.K. Walker, J.P. Harmon, Polysiloxane-based scintillators doped with oligophenylenes: Effect of color centers on radiation stability. *Nucl.*

Instrum. Meth. Phys. Res. B **290**(1), 131–135 (1990). doi:10.1016/0168-9002(90)90351-7

[25] J. Harmon, J. Gaynor, V. Feygelman, J. Walker, Linear polydiorganosiloxanes as plastic bases for radiation hard scintillators. *Nucl. Instrum. Meth. Phys. Res. B* **53**(3), 309–314 (1991). doi:10.1016/0168-583X(91)95619-O

[26] T. Li, C. Zhou, M. Jiang, UV absorption spectra of polystyrene. *Polymer Bulletin* **25**(2), 211–216 (1991). doi:10.1007/BF00310794

[27] N.P. Zaitseva, A.M. Glenn, M.L. Carman et al., Multiple dye interactions in plastic scintillators: Effects on pulse shape discrimination. *Nucl. Instrum. Meth. Phys. Res. A* **978**, 164455 (2020). doi:10.1016/j.nima.2020.164455

[28] A. Quaranta, S. Carturan, M. Cinausero et al., Characterization of polysiloxane organic scintillators produced with different phenyl containing blends. *Mater. Chem. Phys.* **137**, 951–958 (2013). doi:10.1016/j.matchemphys.2012.10.041

[29] T.H. Thomas, T.C. Kendrick, Thermal analysis of polydimethylsiloxanes. I. Thermal degradation in controlled atmospheres. *J. Pol. Sci. Part A-2: Pol. Phys.* **7**(3), 537–549 (2003). doi:10.1002/pol.1969.160070308

[30] D. Barman, K. Narang, R. Parui et al., Review on recent trends and prospects in π-conjugated luminescent aggregates for biomedical applications. *Aggregate* **3**(3), e172 (2022). doi:10.1002/agt2.172

[31] J.B. Birks, *The Theory and Practice of Scintillation Counting*. Pergamon Press, London, 1964.

[32] Y.H. Chen, X.M. Chen, X.D. Zhang et al., Study of n-γ discrimination in low energy range (above 40 keVee) by charge comparison method with a BC501A liquid scintillation detector. *Chin. Phys. C* **38**, 036001 (2014). doi:10.1088/1674-1137/38/3/036001

[33] L. Luo, D. Fang, K. Han et al., Improvement on the linearity response of PandaX-4T with new photomultiplier tube bases. *J. Instrum.* **19**(5), P05021 (2024). doi:10.1088/1748-0221/19/05/P05021

[34] X. Wang, S. Cui, Measurement of PMT charge nonlinearity using the continuous light attenuation method. *J. Instrum.* **18**(12), T12010 (2023). doi:10.1088/1748-0221/18/12/T12010